Electronic Supplementary Material (ESI) for New Journal of Chemistry.

Boron-doped CoP/nitrogen-doped carbon drives enhanced alkaline hydrogen evolution

*Ruru Fu[a], Yun Zhao[*a], Caihong Feng[a], and Qingze Jiao[a,b]*

[a]Beijing Key Laboratory for Chemical Power Source and Green Catalysis, School of Chemistry and Chemical Engineering, Beijing Institute of Technology, South Zhongguancun Street No.5, Haidian District, Beijing 100081, China

[b]School of Materials and Environment, Beijing Institute of Technology, Jinfeng Road No.6, Xiangzhou District, Zhuhai 519085, China

*Corresponding author: zhaoyun@bit.edu.cn

Experimental Section

Materials

Potassium hexacyanocobaltate (III) ($K_3[Co(CN)_6]$, AR), sodium citrate dihydrate ($Na_3C_6H_5O_7 \cdot 2H_2O$, AR), cobalt acetate tetrahydrate ($Co(CH_3COO)_2 \cdot 4H_2O$, AR),sodium borohydride ($NaBH_4$, AR), sodium hypophosphite (NaH_2PO_2, AR), potassium hydroxide (KOH), ethanol (CH_3CH_2OH, AR) were purchased from Shanghai Aladdin Biochemical Technology Co., Ltd. Nafion solution (5 wt%, D-520) was acquired from Alfa Aesar Chemical Co. Ltd. All chemicals were used without further purification.

Characterization

The morphologies and elemental compositions of the samples were observed using scanning electronic microscopy (SEM, Hitachi SU8020) and transmission electronic microscopy (TEM, JEOL JEM1200EX). The crystalline phase of the samples was analyzed using the powder X-ray diffraction (XRD) measurements (Ultima IV, 40 kV, 40 mA, Cu-Kα radiation, 5-80°) at a scanning rate of 10° min^{-1}. The element analysis was analyzed by X-ray photoelectron spectroscopy (XPS, Thermo Scientific K-Alpha). The chemical compositions of the samples were measured by inductively coupled plasma mass spectrometry (ICP-MS, Aglient 7800).

Electrochemical measurements

Electrochemical measurements were conducted on CHI 760E

electrochemical workstation in 1 M KOH solution. 5 mg as-prepared catalysts and 5 mg Super P were dispersed in the mixture of 900 μL ethanol and 100 μL Nafion solution to form a homogeneous ink, and 10 μL of the ink was dropped on the glass carbon electrode (GCE, diameter 5 mm) as the working electrode. A Hg/HgO electrode (0.098 vs. RHE) and graphite rod were used as reference electrode and auxiliary electrode, respectively. All potentials presented were converted to the reversible hydrogen electrode (RHE) and corrected for 95% iR compensation to eliminate the effect of solution resistance. The polarization curves were performed by linear sweep voltammetry (LSV) at a scan rate of 5 mV s^{-1} under rotating at 1600 rpm. The Tafel plots were obtained by the corresponding LSV curves plotted as overpotential versus log j. Electrochemical impedance spectra (EIS) were performed between 0.01 -100 kHz with an amplitude of 5 mV under an applied potential high enough to trigger the HER. The electrochemically active specific area (ECSA) can reflect the number of active sites and be estimated from the electrochemical double-layer capacitance. The C_{dl} was determined by cyclic voltammetry (CV) scans between 0.65 to 0.75 V vs. RHE with different sweep rates (10, 20, 40, 60, 80 and 100 mV s^{-1}). The stability test was assessed by chronopotentiometry for 24 h at about 10 mA·cm^{-2}.

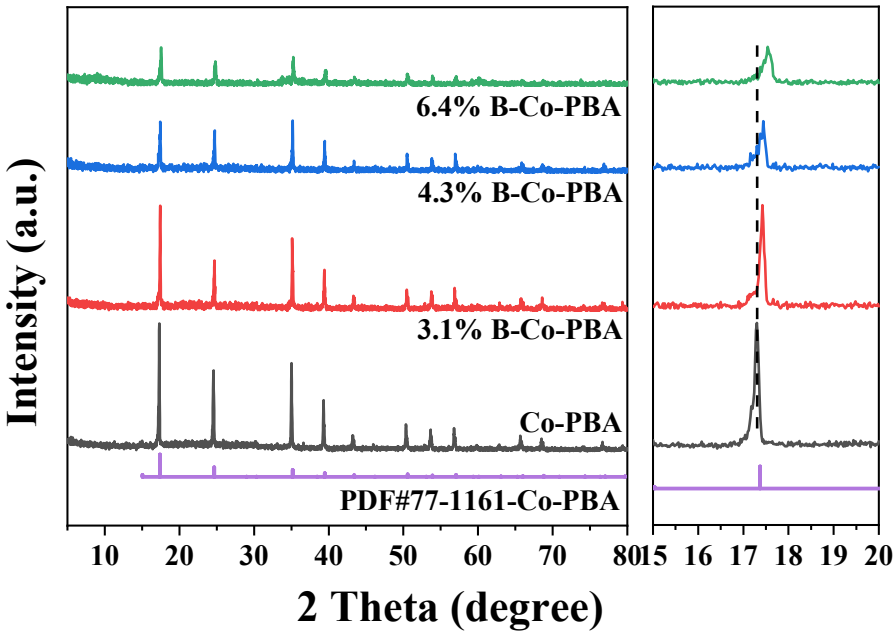

Fig. S1 XRD patterns of Co-PBA and x% B-Co-PBA (x=3.1, 4.3, 6.4)

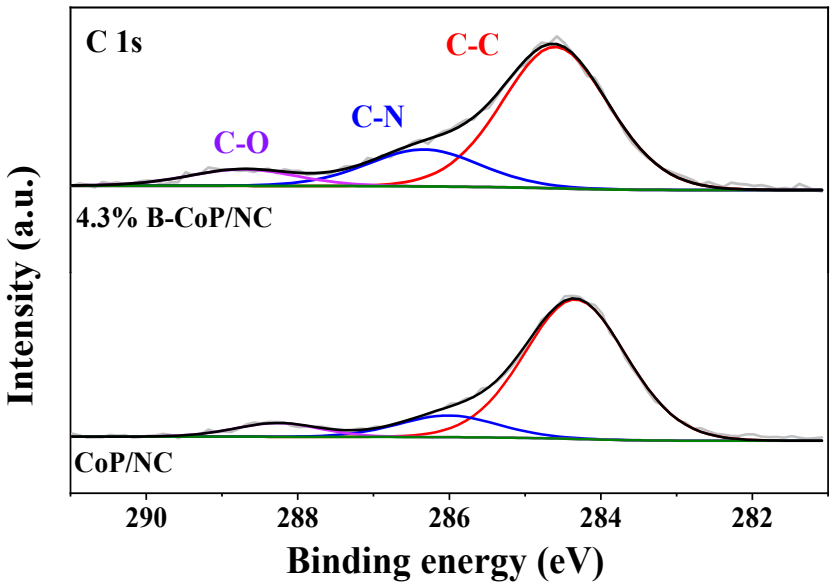

Fig. S2 XPS spectra of C 1s for 4.3% B-CoP/NC.

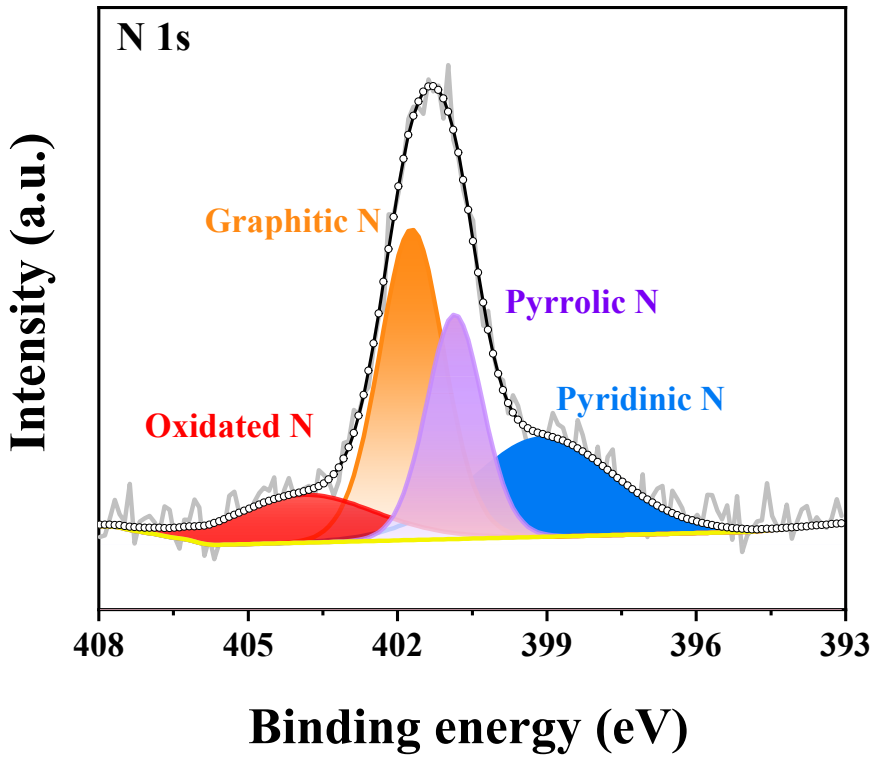

Fig. S3 High-resolution XPS spectra of N 1s of 4.3% B-CoP/NC

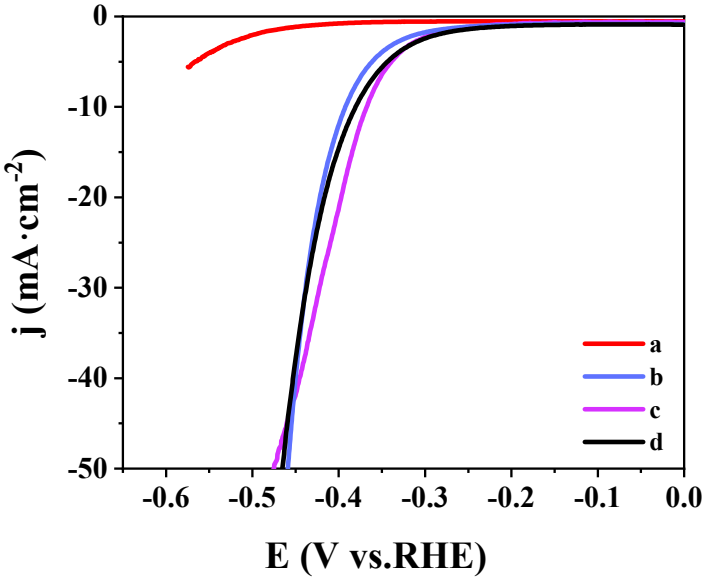

Fig. S4 HER polarization curves of annealed B doped sample without phosphiding process (a: annealed Co-PBA; b: annealed 3.1% B-Co-PBA; c: annealed 4.3% B-Co-PBA; d: annealed 6.4% B-Co-PBA).

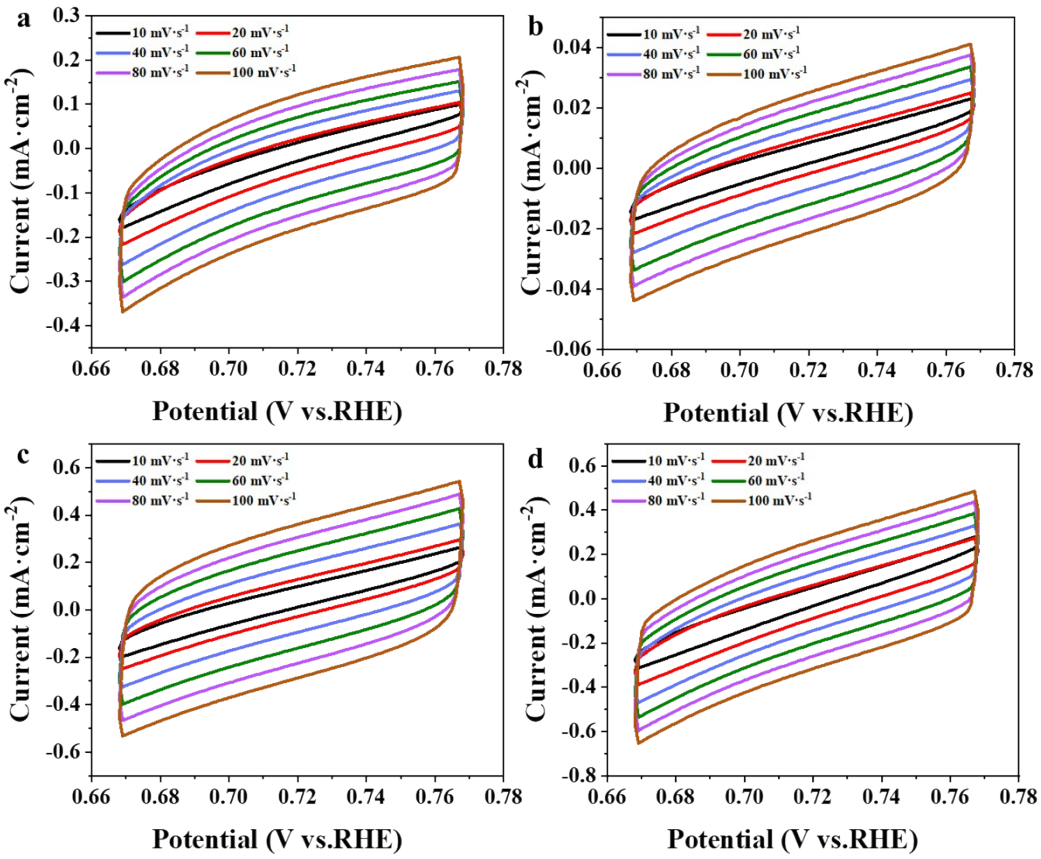

Fig. S5 CVs measurement with various scan rates for (a) CoP/NC, (b) 3.1% B-CoP/NC, (c) 4.3% B-CoP/NC and(c) 6.4% B-CoP/NC in 1 M KOH.

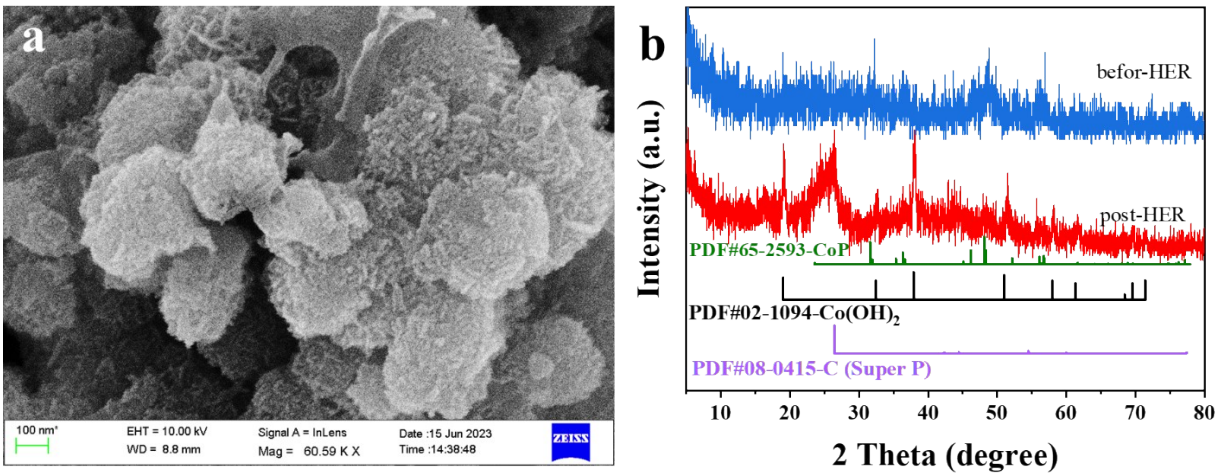

Fig. S6 (a) SEM image and (b) XRD pattern of 4.3% B-CoP/NC after HER stability test

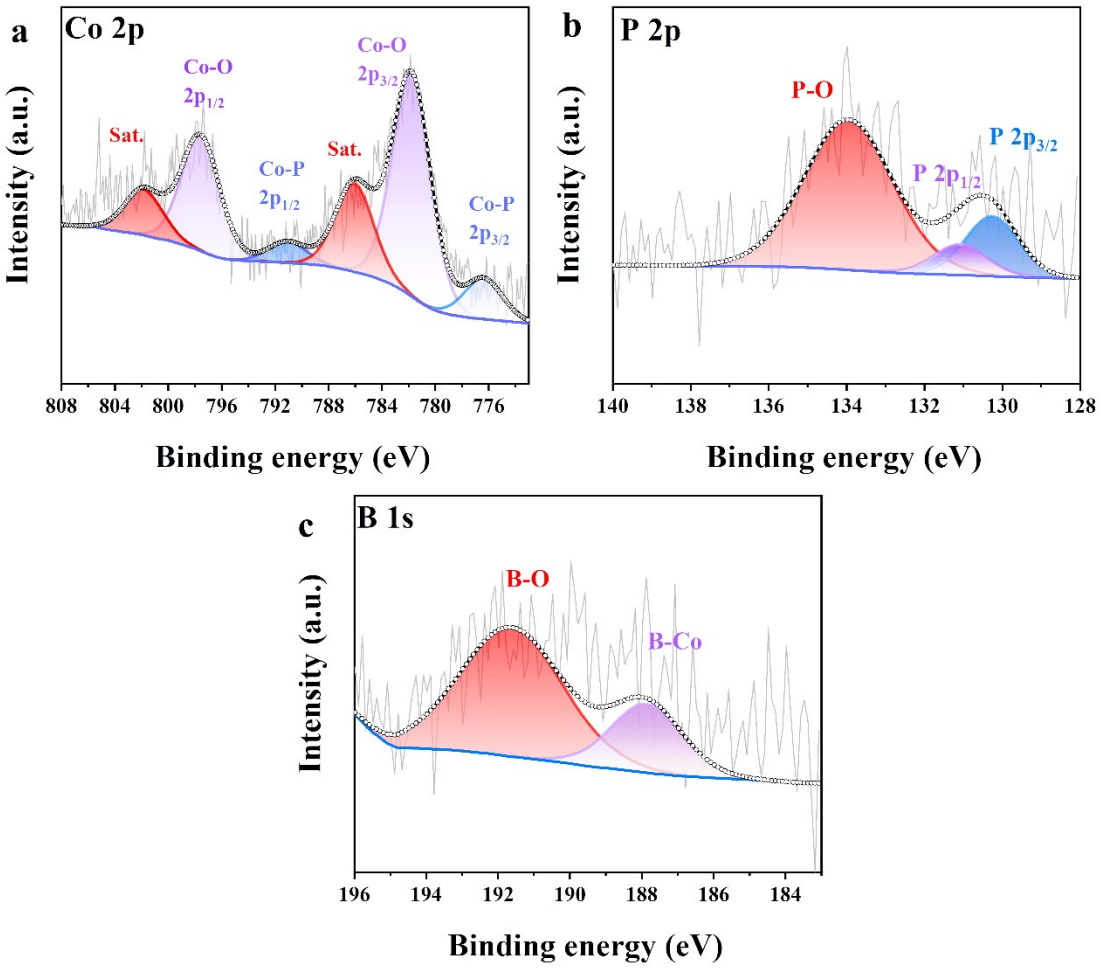

Fig. S7 High-resolution XPS spectra of 4.3% B-CoP/NC after stability test (a) Co 2p, (b) P 2p and (c) B 1s.

Tab. S1 Performance comparison of this work and other HER catalysts.

Catalyst	Electrolyte	Electrode	η (mV)	Tafel Slope (mV dec^{-1})	Ref
B-CoP/NC	1M KOH	Glassy carbon	158@10 mA cm^{-2} 234@100 mA cm^{-2}	67	This Work
Ce-doped CoMoP/ MoP@C	1M KOH	Glassy carbon	188@10 mA cm^{-2}	72.2	1[1]
V-doped CoP	1M KOH	Glassy carbon	235@10 mA cm^{-2}	86.1	2[2]
Ni-doped Co2P/CoP@N−C	1 M KOH	Ni foam	161@10 mA cm^{-2}	94	3[3]
Ni_xCo_yP/Co_2P@NF	1 M KOH	Ni foam	170@100 mA cm^{-2}	67.1	4[4]
Nb-CoP	1 M KOH	Glassy carbon	99@10 mA cm^{-2}	59.4	5[5]
NiCo@BC	1 M KOH	Glassy carbon	209@10 mA cm^{-2}	60	6[6]

1. T. Chen, Y. Fu, W. Liao, Y. Zhang, M. Qian, H. Dai, X. Tong and Q. Yang, *Energy Fuels*, 2021, **35**, 14169-14176.
2. J.-F. Qin, J.-H. Lin, T.-S. Chen, D.-P. Liu, J.-Y. Xie, B.-Y. Guo, L. Wang, Y.-M. Chai and B. Dong, *Journal of Energy Chemistry*, 2019, **39**, 182-187.
3. P. Arunkumar, S. Gayathri and J. H. Han, *ACS Applied Energy Materials*, 2022, **5**, 2975-2992.
4. Y. Zhang, H. Liu, R. Ge, J. Yang, S. Li, Y. Liu, L. Feng, Y. Li, M. Zhu and W. Li, *Sustainable Materials and Technologies*, 2022, **33**, e00461.
5. W. Zou, J. Xiang and H. Tang, *Int. J. Hydrogen Energy*, 2022, **47**, 13251-13260.
6. B. Adegbemiga Yusuf, M. Xie, W. Yaseen, C. Judith Oluigbo, W. Wei, Y. Xu and J. Xie, *ChemElectroChem*, 2021, **8**, 1337-1348.